

**Aperiodic superconducting phase boundary of periodic micronetworks in a magnetic field**

Franco Nori

*Materials Research Laboratory, Physics Department, and National Center for Supercomputing Applications, University of Illinois, Urbana, Illinois 61801*

*and Institute for Theoretical Physics, University of California, Santa Barbara, California 93106\**

Qian Niu

*Physics Department, University of Illinois, Urbana, Illinois 61801*

*and Physics Department, University of California, Santa Barbara, California 93106\**

(Received 28 August 1987)

We study flux quantization in periodic arrays with two elementary cells having an irrational ratio of areas. In particular, we calculate the superconducting-normal phase boundary  $T_c(H)$  and we analyze the origin of its overall and fine structure as a function of the network size. We discuss our theoretical results, exploiting the electronic tight-binding analogy to the Ginzburg-Landau equations, and compare them with the experimental ones.

Micronetworks made of thin superconducting wires,<sup>1</sup> and Josephson junction arrays,<sup>2</sup> exhibit interesting forms of phase diagrams when they are immersed in an external magnetic field. The diamagnetic properties of such micronetworks are very sensitive to the connectedness and the geometry of the multiply connected structure. Fractal,<sup>3</sup> disordered, and quasicrystalline<sup>4,5</sup> geometries have recently been investigated by different groups.

In the present work we study the superconducting-normal phase boundary of new and more complex types of periodic arrays.<sup>6</sup> Since the ratio of the areas of the elementary plaquettes is an irrational number, the system is frustrated at any nonzero field. This basic idea, geometry-induced frustration, has recently been studied in the very interesting work by Behrooz *et al.*<sup>4</sup> and, afterwards, by several other groups.<sup>5</sup> Clearly, the periodic network of Behrooz *et al.* (see Fig. 9 of their long paper<sup>4</sup>) is related to the geometries studied here. The former will be discussed at length somewhere else (numerically and analytically), together with all the geometries studied in the papers by Behrooz *et al.*<sup>4</sup> Our results here only focus on the IBM samples<sup>6</sup> and their phase boundaries. In particular, we study step by step in a progressive way the effect of adding more and more tiles to the basic cells of the samples. This approach allows us to gain insight about the origin of the overall and fine structure present in  $T_c(H)$ . Furthermore, we exploit the electronic tight-binding analogy to the linearized Ginzburg-Landau equations to explain some of the features observed in the phase boundaries.

In order to compute the upper critical field of a superconducting network near the second-order phase boundary, in the context of mean-field theory, we need to solve the linearized Ginzburg-Landau equation. It has been shown<sup>7</sup> that this approach leads, in general, to an eigenvalue problem expressed in terms of the order-parameter values at the nodes. If node  $\alpha$  is linked to  $n$  nodes via strands of length  $L_{\alpha\beta}$  ( $\beta = 1, \dots, n$ ), the basic equation at

node  $\alpha$  is

$$\sum_{\beta=1}^n \Delta_{\beta} e^{iA_{\alpha\beta}} / \sin \left( \frac{L_{\alpha\beta}}{\xi_s} \right) = -\Delta_{\alpha} \sum_{\beta=1}^n \cot \left( \frac{L_{\alpha\beta}}{\xi_s} \right), \quad (1)$$

where  $\Delta_{\beta}$  ( $= |\Delta_{\beta}| e^{i\varphi_{\beta}}$ ) is the value of the order parameter at node  $\beta$ ,  $\xi_s = \xi_0 (T_{co}/\delta T)^{1/2}$  is the coherence length,  $\delta T = T_{co} - T$ ,  $A_{\alpha\beta} = (2\pi/\Phi_0) \int_{\alpha}^{\beta} \mathbf{A} \cdot d\mathbf{l}$  is the circulation of the vector potential  $\mathbf{A}$  along the wire linking  $\alpha$  and  $\beta$ , and  $\Phi_0$  ( $= ch/2e$ ) the elementary flux quantum. For a lattice where  $L_{\alpha\beta} \equiv L$  is the same for all links, Eq. (1) reduces formally to that of a Landau-level structure of a free-electron gas in the same geometry, with the analog of the energy being given by  $Z \cos(L/\xi_s)$ , where  $Z$  is the coordination number of every node.

The geometries considered here are two-dimensional (2D) lattices which correspond to the space groups  $p4gm$  and  $c2mm$  (see Fig. 1). The elementary cells are a triangle and a square with a ratio of areas equal to  $r = A_{sq}/A_{tr} = 4/\sqrt{3}$ . In our calculations  $A_{sq} = 1$ ; therefore the characteristic field corresponding to one flux quantum in the square becomes  $H_{sq} = \Phi_0/A_{sq} = \Phi_0$ . All the  $T_c(H)$

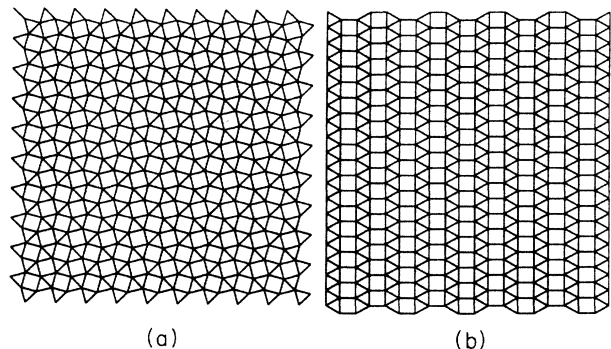


FIG. 1. Two-dimensional networks, with 400 nodes each, denoted by (a)  $p4gm$  and (b)  $c2mm$ .

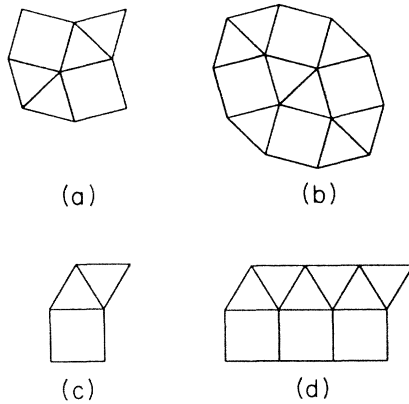


FIG. 2. Small networks, which are denoted here by (a)  $p4gm.9$ , (b)  $p4gm.14$ , (c)  $c2mm.6$ , and (d)  $c2mm.12$ . The small networks  $p4gm.9$  and  $c2mm.6$  are unit cells of the  $p4gm$  and  $c2mm$  lattices, respectively.

plots presented here have the horizontal axis  $H$  measured in units of  $H_{sq} = \Phi_0$ . For simple geometries, such as the square or 2D Fibonacci lattice, the determination of  $T_c(H)$  is greatly simplified since in these cases the original equations on the 2D structure can be mapped into a 1D equation. This is not the case for the lattices considered here since the bonds do not belong to two sets which are perpendicular to each other.

Let us first consider the small networks shown in Fig. 2, which will be denoted here by  $sg.m$ , where  $sg$  is a space group and  $m$  is the number of nodes present in the network;  $p4gm.9$  [Fig. 2(a)] and  $c2mm.6$  [Fig. 2(c)] are unit cells of the  $p4gm$  and  $c2mm$  lattices, respectively. The remaining small networks are larger subsets of the lattices depicted in Fig. 1. Figure 3 shows the transition from a periodic phase boundary [Fig. 3(a)] corresponding to a

single triangular cell, to the nonperiodic ones associated with the  $p4gm.9$  [Fig. 3(b)] and  $p4gm.14$  [Fig. 3(c)] geometries. The maxima of the  $T_c(H)$  curve for the triangular cell (a) are parabolic. However, the local maxima become sharper and sharper when the system size grows. In the large-system limit, 400 nodes in our calculation, the local maxima are cusplike. One-cell effects are responsible for the quadratic maxima, while the cusplike behavior is due to the collective effect of many cells. Also, the maxima in (a) split into several local maxima, in (b) and (c), due to the competition between cells with different areas. Figure 4 shows the  $T_c(H)$  curves for the small networks  $c2mm.6$  and  $c2mm.12$ .

Let us consider the number of cusps present in the  $T_c(H)$  curves depicted in Figs. 3(c) and 4(b). Clearly, the former has more cusps. It is also clear that their respective networks have two mirror-symmetry planes in Fig. 2(b) and no symmetries in Fig. 2(d). The lack of symmetry in the latter one implies that the eigenenergies (we are using the electronic tight-binding analogy of the linearized Ginzburg-Landau equations) tend to avoid each other.<sup>8</sup> Therefore,  $T_c(H)$  will be smooth [Fig. 4(b)]. On the other hand, the presence of two mirror-symmetry planes in the former implies that level crossings, and therefore cusps, coming from eigenenergies associated with different eigensubspaces of the irreducible representation of the Hamiltonian, are highly probable. In summary, the higher the degree of symmetry, the more likely electron levels will cross the largest eigenvalue,  $T_c(H)$ , creating cusps even in small networks. In small networks, downward cusps (which look like V) are due to level crossing, and are very sensitive to the detailed geometry. As the lattice size grows, the originally rounded peaks become sharper and sharper and eventually become upward (i.e.,  $\wedge$ ) cusps. This latter type of cusp comes from the collective effect of the many cells.

The results shown in Figs. 3 and 4 show that short-

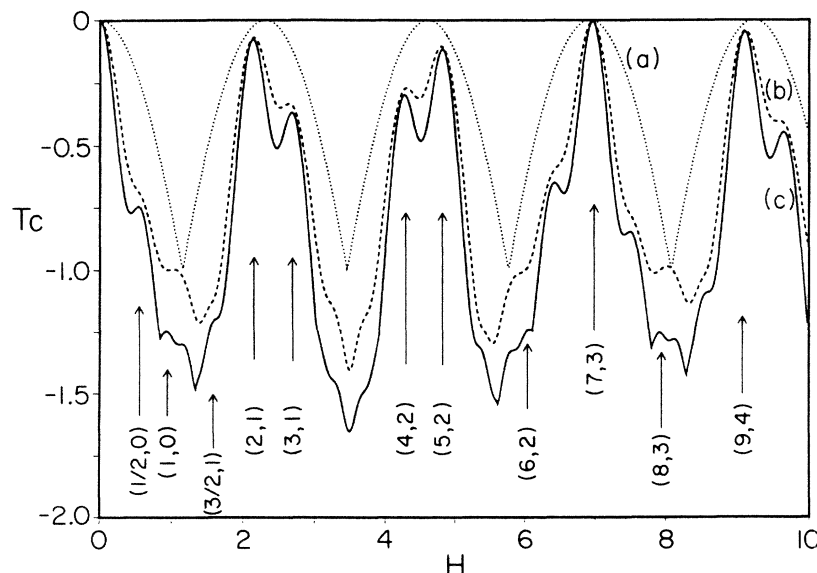


FIG. 3.  $T_c$  (in arbitrary units) vs  $H$  (in units of  $H_{sq} = \Phi_0/A_{sq} = \Phi_0$ ) for the small networks (a) one triangular cell, (b)  $p4gm.9$ , and (c)  $p4gm.14$ .

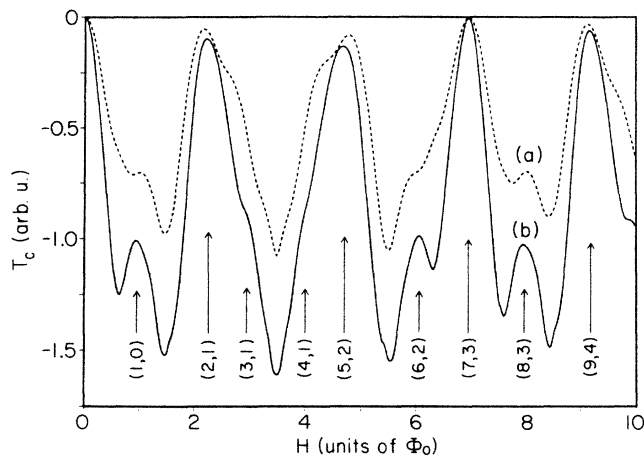


FIG. 4. Phase boundary  $T_c$  (arbitrary units) vs  $H$  (same units as Fig. 3) for the small networks (a)  $c2mm.6$  and (b)  $c2mm.12$ .

range correlations among tiles are responsible for the main overall features in the  $T_c(H)$  curve, while longer-range correlations, a many-tile effect, are responsible for the finer structure. Let  $n_{sq}$  ( $n_{tr}$ ) be the average number of flux quanta in each square (triangle). The average magnetic field on the array can be expressed as

$$H_{av} = H_{sq}(n_{sq} + 2n_{tr}) / (1 + \sqrt{3}/2) = H_p n,$$

where  $H_p = H_{sq} / (1 + \sqrt{3}/2)$  and  $n = n_{sq} + 2n_{tr}$ . Therefore, the arrangements of the flux quanta on the array can be indexed by  $(n_{sq}, n_{tr})$ . Furthermore, the most prominent maxima occur at field strengths associated with  $(n_{sq}, n_{tr}) = (2, 1), (5, 2), (7, 3), (9, 4), \dots$ , where the respective ratios  $n_{sq}/n_{tr} = 2, 2.5, 2.33, 2.25, \dots$  are successive approximants to  $4/\sqrt{3}$ . Some fine structure, in which  $n_{sq}$  is a rational number, has also been indicated.

We have numerically solved the linearized Ginzburg-Landau equations and obtained the  $T_c(H)$  curves, see Fig. 5, for the 400-node networks shown in Fig. 1. We summarize some of the most relevant features of the experimental results and our theoretical phase boundaries. (i)  $T_c(H)$  is not periodic; however, some local maxima do exhibit one period corresponding to  $H_p$ . (ii) The largest maxima correspond to the case when successive rational (approximants to  $r$ ) numbers of flux quanta are found in small and large tiles. At these field strengths,  $\Phi_{sq}/\Phi_{tr}$  approximates the ratio of their areas. (iii) The previously mentioned maxima only approach the zero-field value for  $T_c$  since the frustration cannot be relieved for any nonzero value of the magnetic field. However, the flux lattice can find favorable arrangements which lower its energy close to the original unfrustrated configuration. (iv) The large peaks labeled  $n=4, 5, 8,$  and  $9$  in Fig. 5(a) are due to the effect of the more numerous triangular cells [see Fig. 3(a)]. (v) There is an approximate mirror symmetry at certain values of the magnetic field [Fig. 5(b)]. This effect comes from the fact that the square and the triangle both have phase boundaries with exact mirror symmetries at integer and half-integer values of the reduced magnetic flux. This property carries over approximately to these

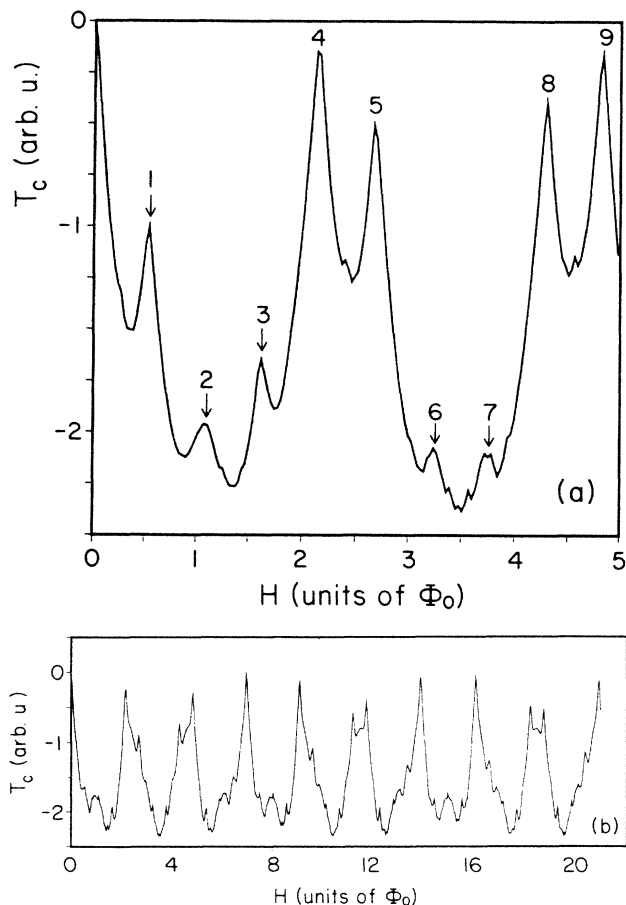


FIG. 5.  $T_c$  (arbitrary units) vs  $H$  (in units of  $H_{sq} = \Phi_0/A_{sq} = \Phi_0$ ) for the (a)  $p4gm$  and (b)  $c2mm$  lattices shown in Fig. 1. The locations of the maxima corresponding to various  $n$  values are indicated by arrows.

more complex lattices. (vi) At low-field values we recover the linear-continuum-limit result (see Fig. 5). This is analogous to the linear behavior of the electron (and hole) Landau levels, and the structure of Landau levels for electrons in free space.

These calculations have been performed for a wide range of magnetic fields. However, to facilitate comparison with the experimental curve by Santhanam *et al.*<sup>6</sup> we have plotted Fig. 5(a) only for small field values. The agreement between them is good. For the  $c2mm$  lattice the agreement is not as good. The origins of these discrepancies can be traced to several factors: (1) imperfections of the fabricated structures (e.g., the nonuniform width of the wires), and (2) the measurement current through the sample may smooth out some of the unobserved fine structure. Although mean-field theory cannot accurately locate the exact value of  $T_c$ , it gives the right dependence with the magnetic field. Moreover, effects coming from our finite-size calculations have been found to be small.

In conclusion, (1) we have studied flux quantization and obtained accurate calculations, without any adjustable parameter, of the superconducting-normal phase boundary for periodic arrays recently studied experimen-

tally,<sup>6</sup> (2) we have found a good agreement between theory and experiment, and we have listed the possible causes of the discrepancies between them, and (3) we have studied the origin of the overall and fine structure of the  $T_c(H)$  curve by analyzing, step by step in a progressive way, the effect of adding more and more tiles to the unit cells of both arrays. Generally speaking, cusps in small networks are due to level crossing (using the electronic tight-binding analogy of the linearized Ginzburg-Landau equations). As soon as the number of cells in the network starts to grow, interactions between cells remove these sharp cusps (i.e., the electronic level crossing between parabolas of noninteracting free electrons is replaced by a gap when many cells interact). On the other hand, smooth (quadratic) maxima in small networks become sharp in larger ones due to the coherent effect coming from many cells. Furthermore, the location and shape of the maxima tends to change in a moderate way when the number of cells continues to increase (since the ratio of areas of the elementary cells tends to dominate its be-

havior). On the other hand, the location and shape of the valleys tend to change somewhat more drastically, e.g., Figs. 3 and 4, since they are more susceptible to the specific geometric arrangement of the cells in the array.

One of us (F.N.) is grateful to E. Fradkin for support and encouragement, to P. Santhanam for his comments and for sending us his unpublished data, and to S. J. Chang, M. Salamon, the National Center for Supercomputing Applications, and the computing center of the Materials Research Laboratory, University of Illinois, for their assistance. This work has been supported in part by the National Science Foundation through Grants No. MRL-DMR-86-12860, No. DMR-84-15063 (University of Illinois), and No. PHY82-17853, supplemented by funds from the National Aeronautics and Space Administration, and by the U.S. Department of Energy through Grant No. DE84-ER-45108 (University of California, Santa Barbara).

\*Permanent address.

<sup>1</sup>B. Pannetier *et al.*, Phys. Rev. Lett. **53**, 1845 (1984); J. Phys. (Paris) Lett. **44**, L853 (1983).

<sup>2</sup>R. A. Webb *et al.*, Phys. Rev. Lett. **51**, 690 (1983); J. Kosterlitz and E. Granato, Phys. Rev. B **34**, 2026 (1986); D. Stroud and Y. Y. Shih, Mater. Sci. Forum **4**, 177 (1985).

<sup>3</sup>J. M. Gordon *et al.* Phys. Rev. Lett. **56**, 2280 (1986); J. M. Gordon and A. M. Goldman, Phys. Rev. B **35**, 4909 (1987).

<sup>4</sup>A. Behrooz, M. Burns, H. Deckman, D. Levine, B. Whitehead, and P. M. Chaikin, Phys. Rev. Lett. **57**, 368 (1986); Phys.

Rev. B **35**, 8396 (1987).

<sup>5</sup>K. Springer and D. Van Harlingen, Phys. Rev. B **36**, 7273 (1987); F. Nori, Q. Niu, E. Fradkin, and S. J. Chang, *ibid.* **36**, 8338 (1987); Pannetier *et al.* (unpublished); J. Chung, M. Y. Choi, and D. Stroud (unpublished).

<sup>6</sup>P. Santhanam, C. C. Chi, and W. W. Molzen, preceding paper, Phys. Rev. B **37**, 2360 (1988).

<sup>7</sup>S. Alexander, Phys. Rev. B **27**, 1541 (1983); R. Rammal, T. C. Lubensky, and G. Toulouse, *ibid.* **27**, 2820 (1983).

<sup>8</sup>J. von Neumann and E. P. Wigner, Phys. Z. **30**, 467 (1929).